

An anisotropic tertiary creep damage constitutive model for anisotropic materials

Calvin M. Stewart^{a,*}, Ali P. Gordon^a, Young Wha Ma^b, Richard W. Neu^c

^a Department of Mechanical, Materials, & Aerospace Engineering, University of Central Florida, USA

^b Department of Mechanical Engineering, Chung Ang University, 221 Huksuk Dongjak, Seoul 156-756, Republic of Korea

^c George W. Woodruff School of Mechanical Engineering, Georgia Institute of Technology, Atlanta, GA 30332-0405, USA

ARTICLE INFO

Article history:

Received 20 April 2010

Received in revised form

30 June 2011

Accepted 30 June 2011

Keywords:

Transversely-isotropic

Continuum damage mechanics (CDM)

Directionally-solidified

Ni-base superalloy

Void induced anisotropy

Multiaxial

ABSTRACT

When an anisotropic material is subject to creep conditions and a complex state of stress, an anisotropic creep damage behavior is observed. Previous research has focused on the anisotropic creep damage behavior of isotropic materials but few constitutive models have been developed for anisotropic creeping solids. This paper describes the development of a new anisotropic tertiary creep damage constitutive model for anisotropic materials. An advanced tensorial damage formulation is implemented which includes both material orientation relative to loading and the degree of creep damage anisotropy in the model. A variation of the Norton-power law for secondary creep is implemented which includes the Hill's anisotropic analogy. Experiments are conducted on the directionally-solidified bucket material DS GTD-111. The constitutive model is implemented in a user programmable feature (UPF) in ANSYS FEA software. The ability of the constitutive model to regress to the Kachanov-Rabotnov isotropic tertiary creep damage model is demonstrated through comparison with uniaxial experiments. A parametric study of both material orientation and stress rotation are conducted. Results indicate that creep deformation is modeled accurately; however an improved damage evolution law may be necessary.

© 2011 Elsevier Ltd. All rights reserved.

1. Introduction

In the power generation and aerospace industries, components such as pressure vessels, pipes, gas turbine disks and vanes, and turbine blades experience high temperatures such that creep deformation will occur. In the case of industrial gas turbines where the cycle duration and maintenance intervals can be in the thousands of hours, and there are drives to increase temperature and pressure, careful selection and accurate prediction of material behavior is paramount; therefore, directionally-solidified (DS) materials have been implemented to minimize intergranular (brittle) creep cracking by alignment of long grains with the first principal stress direction [1]. Typically DS gas turbine blade materials are transversely-isotropic, consisting of a columnar microstructure where there is a plane of “transverse grain (T)” isotropy and an enhanced “longitudinal grain (L)” orientation. Creep and stress-rupture properties are one of the more important variables in the overall life of turbine blades [2].

In the case of welded pressure vessels, welding is a directional solidification process. A single weld bead consists of a single

columnar solidification microstructure. Multi-pass welding (used on pressure vessels) will produce a transversely-isotropic microstructure [3].

In the case of thin-walled pipes used in power plants, considerable work has been focused around isotropic creep damage modeling [4,5]. Literature has demonstrated that strength anisotropy in thin-walled tubular elements is common [6].

Accurate modeling of the creep deformation and damage behavior of transversely-isotropic materials is important. A novel anisotropic creep damage model for transversely-isotropic materials is developed based on the Kachanov-Rabotnov isotropic formulation [7,8]. Experiments are conducted on uniaxial specimen of the bucket material DS GTD-111. The constitutive model is implemented in Finite Element Analysis (FEA) software. A comparison between the experiments, Kachanov-Rabotnov model, and novel constitutive model is conducted. An examination of the strain tensor is provided. A parametric exercise of the constitutive model for various material orientations and states of stress demonstrates functionality.

2. Continuum damage mechanics

A damage mechanism is a manifestation of the degradation of the microstructure of a material and can occur in two forms: transgranular (ductile) damage and intergranular (brittle) damage. Transgranular (ductile) damage arises where slip bands of plasticity

* Corresponding author. 4000 Central Florida Blvd., Bldg. 40 Room 358, Orlando, FL 32816-2450, USA. Tel.: +1 (407) 435 0047.

E-mail address: calvin.stewart@knights.ucf.edu (C.M. Stewart).

form under high stress and low temperature. Intergranular (brittle) damage is a microcracking process at grain boundaries under high temperature and low stress [9]. A number of Continuum Damage Mechanics (CDM) based constitutive models have been developed for creep damage prediction [10]. An early and often cited attempt came from Kachanov [7] and Rabotnov [8] in the form of coupled creep strain rate and damage evolution equations for isotropic materials as follows

$$\dot{\epsilon}_{cr} = \frac{d\epsilon_{cr}}{dt} = A \left(\frac{\bar{\sigma}}{1-\omega} \right)^n \quad (1)$$

$$\dot{\omega} = \frac{d\omega}{dt} = \frac{M\bar{\sigma}^\chi}{(1-\omega)^\phi} \quad (2)$$

where A and n are secondary creep constants, M , χ , and ϕ are tertiary creep damage constants, and $\dot{\epsilon}_{cr}$ and $\bar{\sigma}$ are the equivalent creep strain and von Mises stress respectively [11–13]. This isotropic formulation regards damage as a scalar state variable, ω that accounts for all microstructural degradations exhibited in a material. Numerous specialized variations on this isotropic constitutive model can be found throughout literature [14–20]. The constitutive model has also been generalized for multiaxial states of stress in isotropic materials using elastic compliance tensors and the stress deviator [21].

Literature shows that under creep conditions, intergranular damage must be represented by multiple principal damage variables. Damage can induce an anisotropic creep response [5,22]. Literature shows that damage anisotropy can be identified in two material classes, aluminum-like and copper-like [9,23]. For aluminum-like materials, damage is typically distributed isotropically. Aluminum-like materials with a simple stress state (i.e., uniaxial creep tests) can be modeled with isotropic creep damage models [22–25]. For copper-like materials, damage develops mainly on the plane perpendicular to the first principal stress. Copper-like materials and components undergoing a complex state of stress exhibit damage induced anisotropic creep response which must be accounted for with more robust modeling techniques [26]. Models have been developed that can account for both aluminum-like and copper-like materials, and the range of intermediate behaviors between them [5,27]. These isotropic constitutive models are unable to model anisotropic microstructure materials.

A number of researchers have developed constitutive models for transversely-isotropic materials; however, most formulations do not accurately model intermediate material orientations (when the longitudinal grains are not parallel or perpendicular to the load direction) [3,28,29]. For anisotropic microstructure materials, the effect of material orientation must be included in the both the creep strain rate and damage evolution equations [30].

3. Constitutive model

In order to produce an accurate multiaxial representation of the creep deformation of a transversely-isotropic material it is first necessary to accurately model the uniaxial x_1 - x_2 plane of symmetry and x_3 normal represented by T and L specimen, respectively. Isotropic creep damage models are commonly implemented for simple cases involving uniaxially loaded isotropic materials. First the framework for a secondary creep model for transversely-isotropic materials based on Norton's power law is outlined. Next, an anisotropic tertiary creep damage constitutive model for transversely-isotropic materials based on Kachanov-Rabotnov is given.

3.1. Secondary creep constitutive model

For anisotropic creeping materials, if creep strain rate tensor $\dot{\epsilon}_{ij}$, and Cauchy stress tensor, σ_{ij} , follow Norton's power law, the creep behavior can be expressed as follows

$$\dot{\epsilon}_{ij} = A_{ij}\sigma_{ij}^n \quad (3)$$

where it is assumed that the creep exponent, n , has the same value in all anisotropic principal directions [31]. Using the appropriate equivalent stress function this can be reduced to an equivalent strain function similar to Eq. (1).

$$\dot{\epsilon}_{cr} = A_{aniso} [\tilde{q}(\sigma_{ij})]^n \quad (4)$$

where A_{aniso} is an equivalent creep coefficient of the anisotropic material and $\tilde{q}(\sigma_{ij})$ is equivalent deviatoric stress function. For isotropic creeping materials, A_{aniso} and $\tilde{q}(\sigma_{ij})$ become the isotropic creep coefficient under multiaxial stress state, A , and the equivalent stress, σ_e . In this paper the discussion is confined to a case where the Cartesian coordinate axes coincide with the symmetry axes of creep orthotropy. For a material of creep orthotropy, the equivalent deviatoric stress function $\tilde{q}(\sigma_{ij})$ can be defined as Eq. (5) in analogy to Hill's yield function [32].

$$\tilde{q}(\sigma_{ij}) = \left[F(\sigma_{22} - \sigma_{33})^2 + G(\sigma_{33} - \sigma_{11})^2 + H(\sigma_{11} - \sigma_{22})^2 + 2L\sigma_{23}^2 + 2M\sigma_{13}^2 + 2N\sigma_{12}^2 \right]^{1/2} \quad (5)$$

where, F , G , H , L , M , and N are unitless material constants which describe the current state of creep orthotropy, and σ_{11} , σ_{22} , etc. are stress components. During creep deformation of a material, the state of anisotropy changes; however, it will be assumed that the change in anisotropy is negligible compared with the initial state of anisotropy, as assumed in the anisotropic plastic theory [32]. Namely, the state of anisotropy remains constant. Hence, by substituting Eq. (5) into Eq. (4) and solving for the cases of principal axes of orthotropy ($i = j = 1, 2$, and 3) and shear directions ($i = 2$ and $j = 3$, $i = 3$ and $j = 1$, and $i = 1$ and $j = 2$), expressions for the creep orthotropy parameters can be obtained as shown in Eq. (6) in terms of creep coefficient ratios. In deriving Eq. (6), the equivalent deviatoric stress function in shear directions of $\tau_e = \sigma_e / \sqrt{3}$ was applied as in the isotropic case.

$$\begin{aligned} F &= \frac{1}{2} \left\{ \left(\frac{A_{22}}{A_{aniso}} \right)^{2/n} + \left(\frac{A_{33}}{A_{aniso}} \right)^{2/n} - \left(\frac{A_{11}}{A_{aniso}} \right)^{2/n} \right\}, \\ G &= \frac{1}{2} \left\{ \left(\frac{A_{33}}{A_{aniso}} \right)^{2/n} + \left(\frac{A_{11}}{A_{aniso}} \right)^{2/n} - \left(\frac{A_{22}}{A_{aniso}} \right)^{2/n} \right\}, \\ H &= \frac{1}{2} \left\{ \left(\frac{A_{11}}{A_{aniso}} \right)^{2/n} + \left(\frac{A_{22}}{A_{aniso}} \right)^{2/n} - \left(\frac{A_{33}}{A_{aniso}} \right)^{2/n} \right\}, \\ L &= \frac{3}{2} \left(\frac{A_{23}}{A_{aniso}} \right)^{2/n}, M = \frac{3}{2} \left(\frac{A_{13}}{A_{aniso}} \right)^{2/n}, \text{ and } N = \frac{3}{2} \left(\frac{A_{12}}{A_{aniso}} \right)^{2/n}. \end{aligned} \quad (6)$$

Assume that the orthotropic creeping material has identical properties in both transverse directions. This transversely-isotropic material has three independent stress components. In order to derive these stress components mathematically, a plane consisting of axis 1 and 2 which is perpendicular to axis 3 is defined as an isotropic plane. Derivation of these stress components is similar to that of the orthotropic plastic material [32]. The following relationship among the parameters can be obtained,

$$G = F, N = G + 2H, \text{ and } M = L \tag{7}$$

inserting these relationships into Eq. (6) gives the following

$$A_{11} = A_{22}, \text{ and } A_{23} = A_{13}, \text{ and } 2N = 3 \left(\frac{A_{12}}{A_{\text{aniso}}} \right)^{2/n} \\ = 4 \left(\frac{A_{22}}{A_{\text{aniso}}} \right)^{2/n} - \left(\frac{A_{33}}{A_{\text{aniso}}} \right)^{2/n} \tag{8}$$

Since the creep orthotropy parameters were defined in terms of the ratios of the creep coefficients as shown in Eq. (6), it can be argued that the equivalent creep coefficient A_{aniso} be equal to A_{33} on the longitudinal direction which is perpendicular to the 1–2 plane (i.e., transverse microstructure plane). Hence, the equivalent deviatoric stress function for the transversely-isotropic creeping material becomes as follows,

$$\tilde{q}(\sigma_{ij}) = \left[\frac{1}{2}(\sigma_{22} - \sigma_{33})^2 + \frac{1}{2}(\sigma_{33} - \sigma_{11})^2 + \left\{ \left(\frac{A_{22}}{A_{33}} \right)^{2/n} - \frac{1}{2} \right\} \right. \\ \times (\sigma_{11} - \sigma_{22})^2 + 3 \left(\frac{A_{13}}{A_{33}} \right)^{2/n} \sigma_{23}^2 + 3 \left(\frac{A_{13}}{A_{33}} \right)^{2/n} \sigma_{12}^2 \\ \left. + \left\{ 4 \left(\frac{A_{22}}{A_{33}} \right)^{2/n} - 1 \right\} \sigma_{12}^2 \right]^{1/2} \tag{9}$$

Consequently, for the transversely-isotropic material the equivalent deviatoric stress function can be determined if only three coefficients, A_{22} (transverse specimen), A_{33} (longitudinal specimen) and A_{13} (45°-oriented specimen) are known. Then, creep behavior of the transversely-isotropic material can be predicted as follows

$$\dot{\epsilon}_{cr} = A_{33} [\tilde{q}(\sigma_{ij})]^n \tag{10}$$

3.2. Tertiary creep damage constitutive model

The novel anisotropic tertiary creep damage model for transversely-isotropic materials is based on the isotropic Kachanov-Rabotnov creep damage constitutive model [7,8]. The influence of the state of damage, ω is accounted for via the effective (net) stress tensor, $\tilde{\sigma}$. A number of formulations for the effective stress have been proposed [9]. Murakami [25] and Murakami and Ohno [33] proposed the symmetric effective (net) stress, $\tilde{\sigma}$ and damage applied, Ω as

$$\Omega = (\mathbf{I} - \omega)^{-1}, \\ \tilde{\sigma} = \frac{1}{2}(\sigma\Omega + \Omega\sigma), \tag{11}$$

where σ is the Cauchy stress tensor and Ω is damage applied.

For anisotropic materials, the orientation of the material grain structure relative to the general coordinates system can significantly alter the damage developed. Thus to account for material orientation the material damage constants need to be formulated into a tensor that alters each tensorial term based on a material orientation vector,

\mathbf{v} where the vector represents the direction of longitudinal grains. The rotated damage constant tensor, \mathbf{B} is defined here as

$$\mathbf{B} = [M_2(\sigma_{\text{Hill}})^{\chi_2} (\mathbf{I} - \mathbf{v}\mathbf{v}^T) + M_1(\sigma_{\text{Hill}})^{\chi_1} (\mathbf{v}\mathbf{v}^T)], \tag{12}$$

where M_1, M_2, χ_1, χ_2 are damage constants and σ_{Hill} is the Hill equivalent stress [32] from the Cauchy stress defined as

$$\sigma_{\text{Hill}} = \sqrt{\mathbf{s}^T \mathbf{M} \mathbf{s}} \\ \mathbf{s} = [\sigma_{11} \quad \sigma_{22} \quad \sigma_{33} \quad \sigma_{12} \quad \sigma_{23} \quad \sigma_{13}]^T \\ \mathbf{M} = \begin{bmatrix} G+H & -H & -G & 0 & 0 & 0 \\ -H & F+H & -F & 0 & 0 & 0 \\ -G & -F & F+G & 0 & 0 & 0 \\ 0 & 0 & 0 & 2N & 0 & 0 \\ 0 & 0 & 0 & 0 & 2L & 0 \\ 0 & 0 & 0 & 0 & 0 & 2M \end{bmatrix} \tag{13}$$

where \mathbf{s} is the vector form of the Cauchy stress tensor, σ and \mathbf{M} is the Hill compliance tensor consisting of the F, G, H, L, M , and N unitless material constants that can be obtained from creep tests [34]. The rotated damage constant tensor, Φ is defined as

$$\Phi^R = [\phi_2(\mathbf{I} - \mathbf{v}\mathbf{v}^T) + \phi_1(\mathbf{v}\mathbf{v}^T)] \\ \Phi = \text{ABS}(\Phi^R) \text{ or } \Phi_{ij} = |\Phi_{ij}^R| \tag{14}$$

where ϕ_1 , and ϕ_2 are damage constants. The rotated damage constant tensor, Φ is used as an elementwise exponent in later mathematics so it is necessary to ensure each element remains positive. The ABS function is introduced which represents an elementwise absolute value of the argument tensor. This is necessary to prevent possible inversion in later analysis that would depend on the selected plane of isotropy. The rotated damage constant tensors allow the creep material properties to be directly related to the orientation of the material grain structure.

In the isotropic damage formulation Eq. (2), it is observed that previous scalar-valued damage is related by $(1 - \omega)^{-\phi}$. An equivalent tensor form is produced by use of the elementwise Schur (or Hadamard) power of the damage applied tensor, Ω and the rotated damage constant tensor, Φ as follows

$$\mathbf{D} = \overrightarrow{\Omega^\Phi} = \Omega^{\circ(\Phi)} \\ \mathbf{D} = \begin{bmatrix} \Omega_{11}^{\Phi_{11}} & \Omega_{12}^{\Phi_{12}} & \Omega_{13}^{\Phi_{13}} \\ \Omega_{21}^{\Phi_{21}} & \Omega_{22}^{\Phi_{22}} & \Omega_{23}^{\Phi_{23}} \\ \Omega_{31}^{\Phi_{31}} & \Omega_{32}^{\Phi_{32}} & \Omega_{33}^{\Phi_{33}} \end{bmatrix} \tag{15}$$

where the convenient tensor, \mathbf{D} is later implemented in the damage rate tensor [35,36]. To account for both aluminum and copper-like, the damage control variable, γ is introduced. This term is applied in the first principal stress influence tensor as follows

$$\mathbf{X} = [(1 - \gamma)\mathbf{I} + \gamma(\mathbf{n}_1 \mathbf{n}_1^T)] \\ 0.0 \leq \gamma \leq 1.0 \tag{16}$$

where \mathbf{n}_1 represents the first principal stress direction vector. When $\gamma = 0.0$ isotropic damage is isotropically distributed while when $\gamma = 1.0$ damage induced anisotropy is allowed to occur.

Table 1
Nominal chemical composition (wt.%) of DS GTD-111 superalloy [37].

Element	Cr	Co	Al	Ti	W	Mo	Ta	C	Zr	B	Fe	Si	Mn	Cu	P	S	Ni
Min	13.7	9.0	2.8	4.7	3.5	1.4	2.5	0.08	0.005	–	–	–	–	–	–	–	Bal.
Max	14.3	10.0	3.2	5.1	4.1	1.7	3.1	0.12	0.040	0.020	0.35	0.3	0.1	0.1	0.015	0.005	Bal.

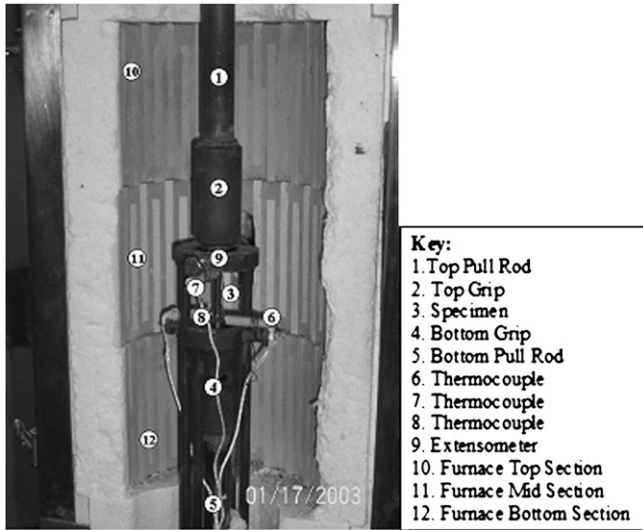


Fig. 1. Creep test rig.

$$\dot{\epsilon}^{cr} = A_{aniso} \bar{\sigma}_{Hill}^{n_{aniso}} \frac{\mathbf{M}\mathbf{s}}{\sigma_{Hill}}, \quad (18)$$

where A_{aniso} , n_{aniso} are secondary creep material constants found via creep tests, \mathbf{M} is the Hill compliance tensor, \mathbf{s} is the Cauchy stress vector, and $\bar{\sigma}_{Hill}$ is the Hill equivalent (net) stress due to the effective stress tensor, $\bar{\sigma}$. To ease the implementation of the model into finite element code, the symmetric stress and strain tensors are converted back and forth to stress and strain vectors (e.g. $\bar{\sigma} \Leftrightarrow \bar{\mathbf{s}}$, $\epsilon^{cr} \Leftrightarrow e^{cr}$). Material rotation can be performed in the creep strain rate equation as follows

$$\dot{\epsilon}^{cr} = A_{aniso} \sqrt{\bar{\mathbf{s}}^T \mathbf{TMT}^T \bar{\mathbf{s}}}^{n_{aniso}} \frac{\mathbf{TMT}^T \mathbf{s}}{\sqrt{\mathbf{s}^T \mathbf{TMT}^T \mathbf{s}}} \quad (19)$$

where \mathbf{T} represents a material orientation transformation tensor about the x_1 axis of the form

$$\mathbf{T} = \begin{bmatrix} 1 & 0 & 0 & 0 & 0 & 0 \\ 0 & \cos(\alpha)^2 & \sin(\alpha)^2 & 0 & 0 & \cos(\alpha)\sin(\alpha) \\ 0 & \sin(\alpha)^2 & \cos(\alpha)^2 & 0 & 0 & -\cos(\alpha)\sin(\alpha) \\ 0 & 0 & 0 & \cos(\alpha) & -\sin(\alpha) & 0 \\ 0 & 0 & 0 & \sin(\alpha) & \cos(\alpha) & 0 \\ 0 & -2\cos(\alpha)\sin(\alpha) & 2\cos(\alpha)\sin(\alpha) & 0 & 0 & \cos(\alpha)^2 - \sin(\alpha)^2 \end{bmatrix}. \quad (20)$$

To produce the damage rate tensor, $\dot{\omega}$, a multiplicative superposition of the rotated damage constant tensor, \mathbf{B} and the convenient tensor, \mathbf{D} which both account for material orientation is performed. This is followed by a symmetric product with the first principal stress influence tensor, \mathbf{X} . The elementwise Schur (or Hadamard) product is used

$$\dot{\omega} = \frac{1}{2} [(\mathbf{B} \circ \mathbf{D}) \cdot \mathbf{X} + \mathbf{X} \cdot (\mathbf{B} \circ \mathbf{D})] \quad (17)$$

$$\mathbf{B} \circ \mathbf{D} = \begin{bmatrix} B_{11}D_{11} & B_{12}D_{12} & B_{13}D_{13} \\ B_{21}D_{21} & B_{22}D_{22} & B_{23}D_{23} \\ B_{31}D_{31} & B_{32}D_{32} & B_{33}D_{33} \end{bmatrix}$$

The \mathbf{B} and \mathbf{D} tensors are both rotations of the material orientation [35,36]. As discussed earlier, undesirable terms develop in tensor \mathbf{D} . The Schur product with \mathbf{B} eliminates them. The damage rate tensor is coupled with the anisotropic creep strain rate equation defined as follows

4. Experiments

The subject material for this study is DS GTD-111, a directionally-solidified Ni-based superalloy commonly used for first and second row blades and vanes of gas turbines. It has a columnar-grained microstructure that manifests transversely-isotropic behavior. The longitudinal axis of the grains is associated with axis x_3 , while the transverse plane is x_1-x_2 . The nominal chemical composition in weight percentage is given in Table 1. The superalloy DS GTD-111 is a dual phase $\gamma-\gamma'$ FCC material, where the γ matrix is FCC austenitic Nickel (Ni), and the primary and secondary γ' precipitated particles are $L1_2$ structured nickel-aluminate (Ni_3Al) with a bimodal distribution [38]. Additionally, $\gamma-\gamma'$ eutectic, carbides and small amounts of topological close-packed phases σ , δ , η and laves are found in the material [38,39]. The creep deformation and rupture test were performed to ASTM standard E-139-96 [40]. Specimens were machined with gage lengths and diameters of 25.4 and 4.064 mm respectively. A lever-type, dead-weight creep machine was used during testing with a ratio of the lever arm of 20:1 as shown in Fig. 1. Test were

Table 2
Creep deformation and rupture data for DS GTD-111 [38].

	Temperature (°C)	Stress MPa	Rupture Strain (%)	Rupture Time (hr)	A (hr ⁻¹)	n	M (MPa ⁻ⁿ hr ⁻¹) x10 ⁻¹¹	χ	ϕ
L	871	241	18.8	2149.0	5.764E-21	6.507	96.015	2.022	7.161
L	871	289	11.7	672.2	5.764E-21	6.507	131.010	2.054	9.698
T	871	241	7.6	980.2	3.480E-21	6.516	263.010	2.098	2.296
T	871	289	5.1	635.3	3.480E-21	6.516	345.840	1.919	6.823
45°	871	244	14.1	68.7	1.374E-23	7.6	53.286	2.156	20.933
45°	871	244	3.8	62.5	1.374E-23	7.6	53.286	2.156	20.933
45°	982	145	9.1	301.7	1.374E-23	7.6	53.286	2.156	20.933

Table 3
Hill constants for DS GTD-111 at 871 °C.

F	G	H	L	M	N
0.5	0.5	0.3866	1.6413	1.6413	1.2731

performed on longitudinal (L), transverse (T), and 45°-oriented specimen. A list of the creep deformation and rupture tests with secondary and tertiary creep damage constants is provided in Table 2. In all cases, the primary creep that arose was small compared to the final rupture strain and is neglected. The micro-structure of all the samples will be left for future work.

5. Results

Previous research using the isotropic Kachanov-Rabotnov constitutive model has produced both secondary and tertiary creep damage constants that can be used directly in the novel constitutive model. The novel anisotropic tertiary creep damage constitutive model requires material constants found through uniaxial creep test in L, T, and 45°-orientations. This is due to the use of Hill’s analogy as both a compliance tensor and equivalent stress in the creep strain rate Eq. (19). To determine the Hill constants, the creep strain rate, Eq. (19), is taken with the damage rate, Eq. (17), disabled via $M_1 = 0.0$ and $M_2 = 0.0$. Various stress transformations and material orientation transformations (about the x_1 normal) are performed. The Hill constants are found to be dependent on the uniaxial Norton-power law for L, T, and 45°-oriented specimen. Subsequently, the Hill constants can be referred back to the minimum strain rates found for L, T, and 45°-oriented specimen. For this study, L, T, and 45°-oriented specimen creep tests were conducted at a temperature of 871 °C and 289 MPa uniaxial load. The Hill constants for DS GTD-111 required by the novel anisotropic creep damage formulation under these conditions are found in Table 3.

Verification of the secondary creep behavior can be achieved using the creep strain rate, Eq. (19), with the damage rate, Eq. (17), disabled. In general, the secondary creep response of the material is controlled by the A_{aniso} , n_{aniso} and Hill constants $F, G, H, L, M,$ and N . Disabling damage ($M_1 = M_2 = 0.0$) leads to the minimum creep

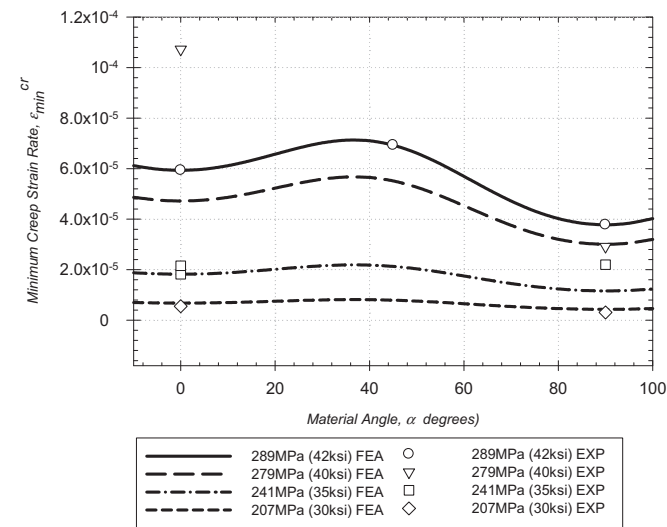


Fig. 2. Material orientation study of x_3 normal minimum creep strain rate at 871 °C for various DS Ni-based materials.

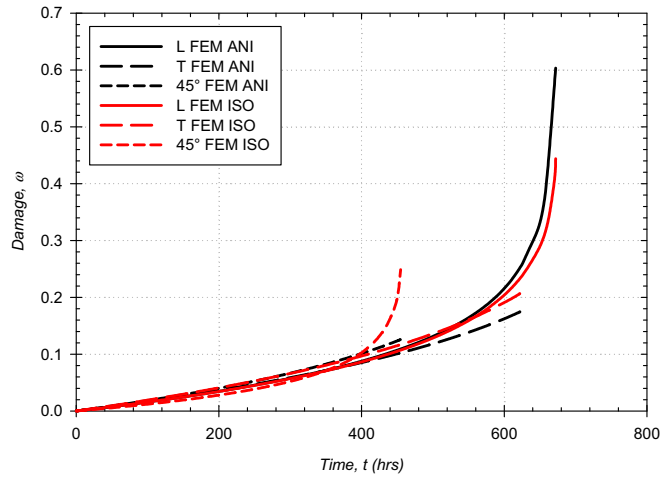


Fig. 3. Damage evolution on the x_3 normal of the isotropic and novel anisotropic creep damage formulations under 289 MPa uniaxial load and 871 °C.

strain rates found in Fig. 2. The observed curve follows the trend expected of a Hill potential based model compared to other DS Ni-based superalloys [41–44]. The FEM prediction of minimum creep strain rates pass through the known rates for L, T, and 45°-oriented specimen at 289 MPa. The material behavior observed in the 279 MPa experiment at $\alpha = 0.0^\circ$ is inconsistent with the study response. Pre-existing flaws in the specimen account for the observed high minimum creep strain rate.

Accurate estimates of damage evolution lead to high quality fits of the creep deformation data. For these purposes, the damage rate Eq. (17) is enabled. Simulations of L, T, and 45°-oriented specimens are executed and compared with those developed using the isotropic creep damage formulation. Fig. 3 shows that the novel anisotropic formulation produces similar damage evolution to the isotropic Kachanov-Rabotnov damage evolution for L and T-oriented specimen; however, the behavior of the 45°-oriented specimen is not accurately modeled. This disconnect is expected. Not directly including the tertiary creep damage constants associated with the 45°-oriented specimen will naturally lead to a less than ideal estimation of damage evolution when compared to the

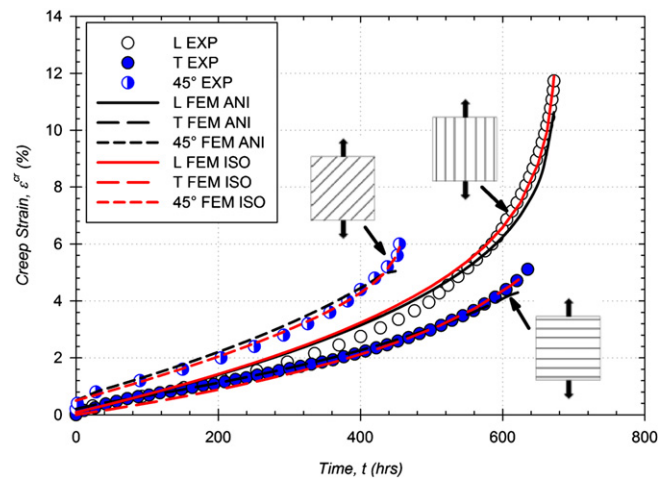


Fig. 4. Creep deformation on the x_3 normal of novel anisotropic and isotropic creep damage formulations compared with creep test data for DS GTD-111 under 289 MPa uniaxial load and 871 °C.

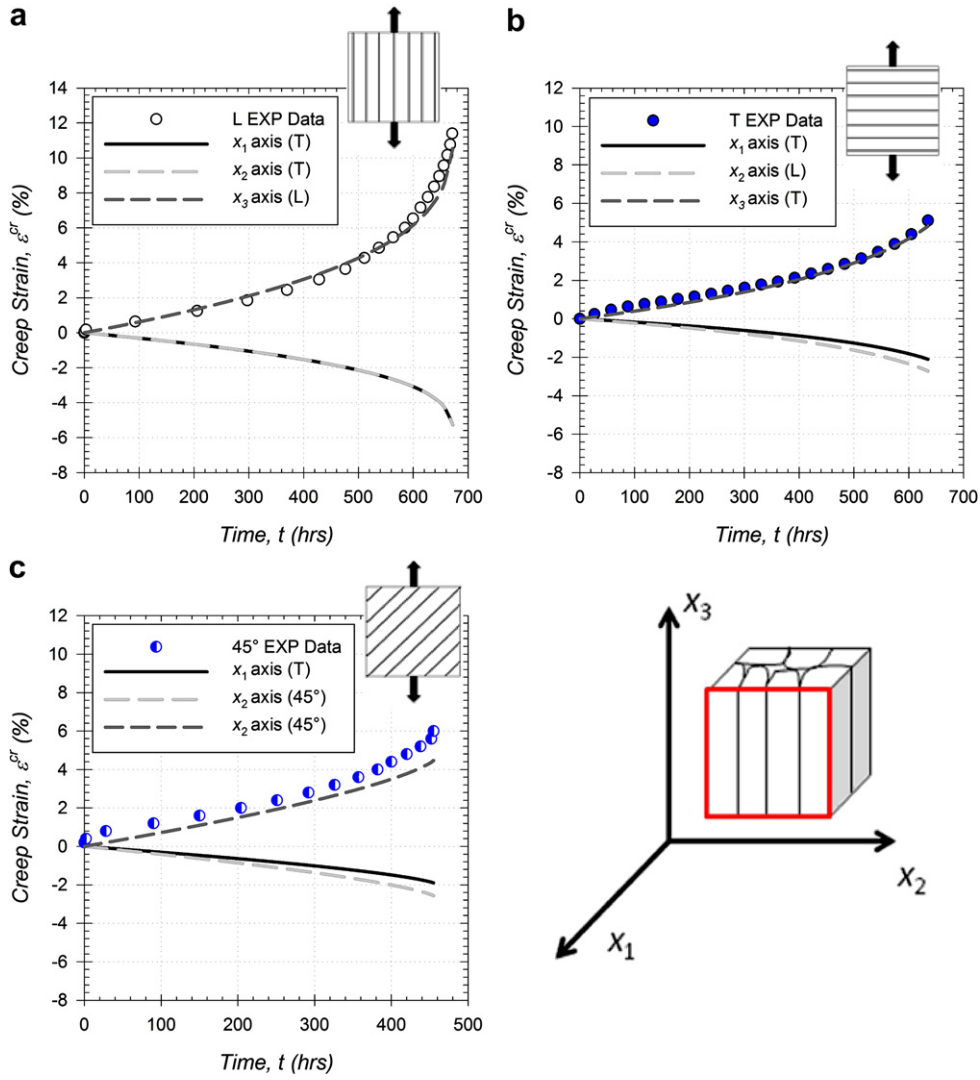


Fig. 5. Components of the creep deformation using the novel anisotropic creep damage formulation for (a) L, (b) T, and (c) 45°-oriented specimen under 289 MPa uniaxial load and 871 °C (note: primary creep is neglected).

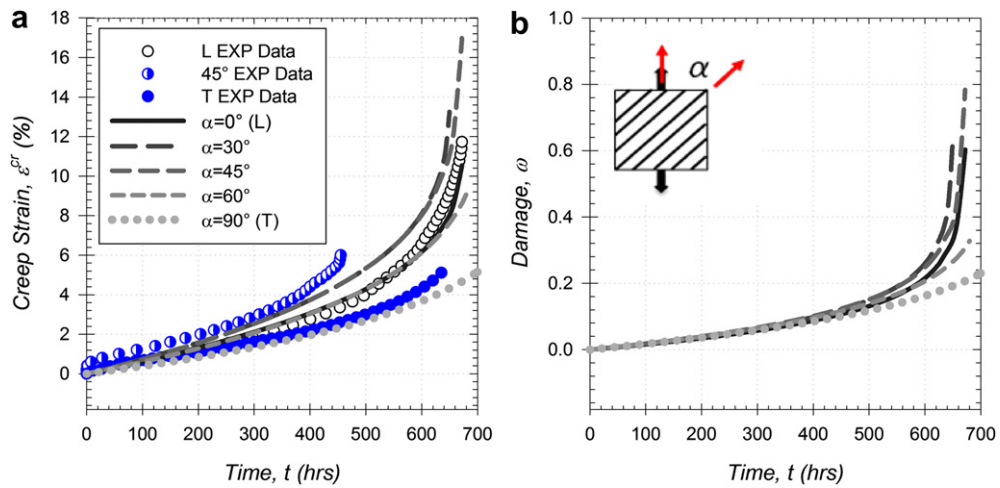


Fig. 6. Material orientation study (a) creep deformation and (b) damage evolution on the x_3 axis (note: $\gamma = 0.0$).

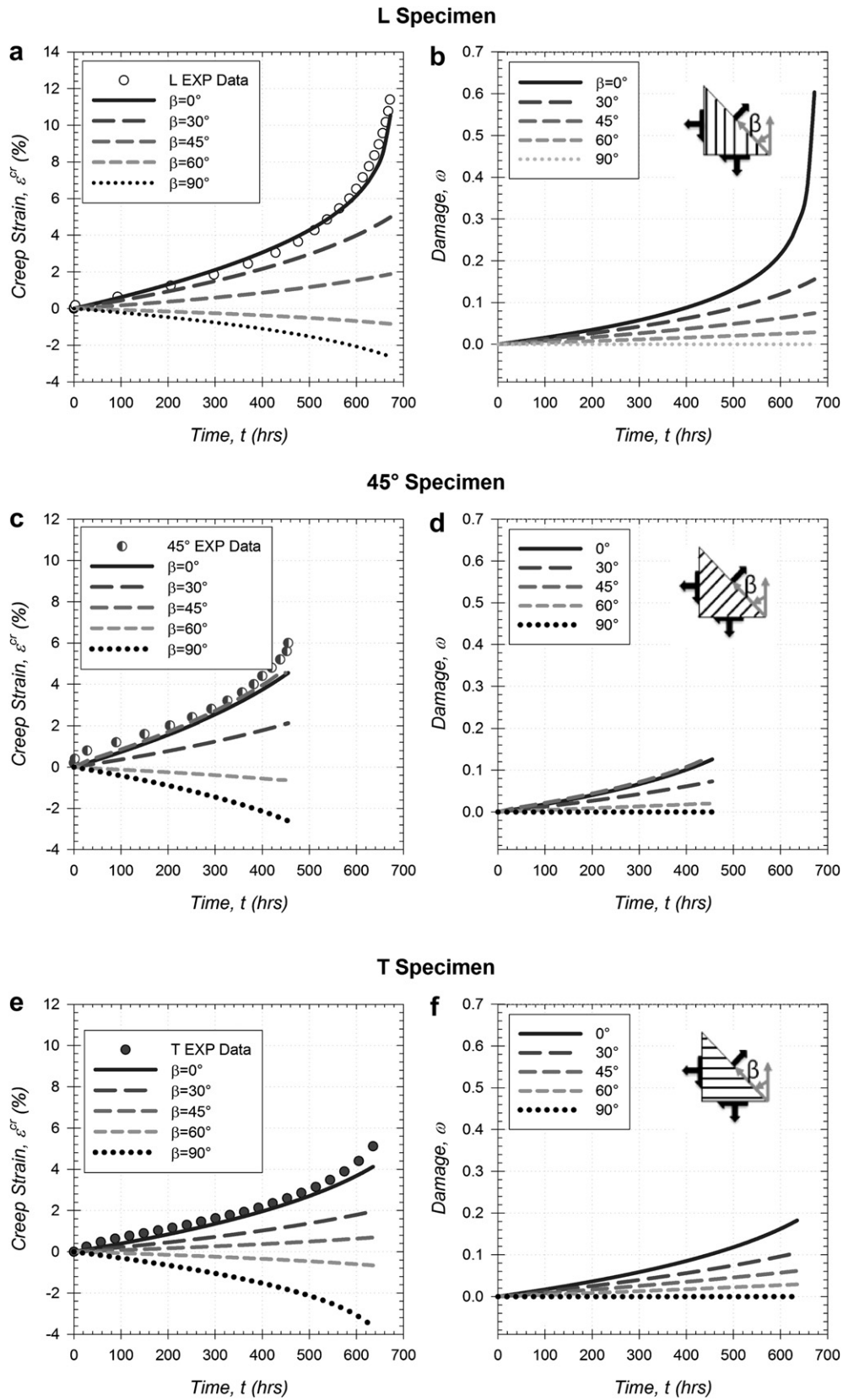


Fig. 7. Stress transformation study for an L and T specimen creep strain (a) & (b) respectively.

isotropic creep damage model. The damage behavior embedded in the novel anisotropic model considers a linear relationship between the L and T-oriented specimen based on material orientation transformation; however, the behavior of DS GTD-111 exhibits a maximized creep strain rate at an orientation between 35° and 45°. While, the predicted damage evolution is not necessarily the same, it is found through examination of the available creep tests data that only slight tertiary creep behavior is found at 45° allowing for a good prediction of the creep strain rate at this orientation.

With the aid of available the creep test data, the creep strain versus time from experimental data is compared with both isotropic and novel anisotropic creep damage formulations. Fig. 4 shows the novel anisotropic formulation performs very well in modeling the creep test experimental data. The accurate prediction of creep strain for a 45°-oriented specimen demonstrates that despite a damage evolution that diverges from the isotropic solution, the novel anisotropic creep damage formulation can accurately predict the creep deformation that develops in transversely-isotropic materials under arbitrary material orientations. Thus the relationship between creep behavior, material orientation, and state of stress are taken into account.

The tensor creep strain behavior of the novel anisotropic creep damage model is of high importance. An accurate creep strain tensor for the subject material proves considerably improved estimations of creep deformation for directionally-solidified components compared to the isotropic creep damage formulation.

Assuming $\gamma = 0.0$, the creep strain tensor response of L, T, and 45°-oriented specimens are presented in Fig. 5. In the case of an L specimen (Fig. 5a), the creep strains found on the x_1 and x_2 normals are equivalent. This is suitable as it shows that isotropy is found on the x_3 axis as expected of an L specimen. In the case of a T specimen (Fig. 5b), the creep strain on the x_2 normal is higher than what develops on the x_3 normal. This is suitable because isotropic behavior is now found on the x_1 - x_3 plane. The L grains produce a higher creep strain rate thus the x_2 normal is higher than the x_3 normal. In the case of a 45°-oriented specimen (Fig. 5c), the creep behavior on the x_2 normal and x_3 normal is the same, however; due to uniaxial loading the creep strain that develops in the x_2 normal is compressive due to the deviatoric response.

In the case of the isotropic creep damage formulation, most FEM codes generalize a full strain tensor via isotropic material properties [45]. In the case of a transversely-isotropic material this would not produce an accurate result. Thus, the novel anisotropic model is found to produce a more accurate strain tensor.

6. Parametric study

A parametric study of the damage and creep strain that develops on the x_3 normal under different material orientations about the x_1 axis was conducted. Under 289 MPa tensile loading and 871 °C, the damage evolution and creep deformation is shown in Fig. 6. In case of creep deformation that difference in creep strain rates between the various orientations follows the material behavior fairly well. In the case of damage evolution, some shortcomings are noticed. Particularly that the trajectory of damage evolution of intermediate orientations does not change much compared to the L and T-oriented specimen. This would produce rupture predictions that do not follow experimental trends. When damage evolution is maximized, the creep deformation is minimal.

A parametric study of the damage and creep strain that develops on the x_3 normal under different stress transformations on L, 45°, and T-oriented specimen was performed. The stress transformation takes the following form

$$\sigma' = \mathbf{Q}\sigma\mathbf{Q}^T = \begin{bmatrix} 0 & 0 & 0 \\ 0 & 0 & 0 \\ 0 & 0 & \sigma_0 \end{bmatrix}$$

$$\mathbf{Q} = \begin{bmatrix} 1 & 0 & 0 \\ 0 & \cos(\beta) & \sin(\beta) \\ 0 & -\sin(\beta) & \cos(\beta) \end{bmatrix} \quad (21)$$

where rotation occurs about the x_1 axis and σ_0 equals 289 MPa. It should be noted that $\gamma = 1.0$, thus the material is assumed to behave like a fully anisotropic damaging material where damage coincides with the first principal stress direction. In all three specimen, the damage reduces to zero as stress transformed from fully on the x_3 normal to the x_2 normal. In the case of creep strain, all three specimens at $\beta = 0.0$ begin at earlier predicted creep strain rates (Fig. 7); however, due to \mathbf{TMT}^T s found in the creep strain rate Eq. (19), at a certain angle between 45° and 60°, tensile creep deformation changes to a compressive deformation due to the deviatoric response. Further examination of shear creep terms finds that the novel anisotropic model is able to account for elongation and angular distortions.

7. Conclusions

It was observed that the aforementioned constitutive model performs well at predicting the creep deformation behavior of a directionally-solidified Ni-based superalloy. The constitutive model was found to accurately, predict the creep deformation of L, 45°, and T-oriented uniaxial specimen of DS GTD-111. Additionally, parametric material orientation and stress rotation simulations inform that the creep strain model can account for multiaxial states of stress and intermediate orientations. In terms of modeling damage, damage evolution at intermediate orientation was found to not correspond well with experimental trends. A better damage evolution model would be necessary to produce accurate rupture time predictions and damage contour plots. Future work will focus on normalization of the damage criterion in all orientations to unity and developing an improved damage evolution model.

Acknowledgments

Calvin Stewart is thankful for the support of a Mcknight Doctoral Fellowship through the Florida Education Fund. Ali P. Gordon recognizes the support of the Florida Center for Advanced Aero-Propulsion (FCAAP).

References

- [1] National Research Council (U.S.). Committee on materials for large land-based gas turbines. Materials for large land-based gas turbines. US: National Academy Press; 1986.
- [2] Pridemore WD. Stress-rupture characterization in nickel-based superalloy gas turbine engine components. Journal of Failure Analysis and Prevention 2008; 8(3):281–8.
- [3] Naumenko K, Altenbach H. A phenomenological model for anisotropic creep in a multipass weld metal. Archive of Applied Mechanics 2005;74(11–12): 808–19.
- [4] Ohno N, Mizuno T, Kawaji H, Okada I. Multiaxial creep of a nickel-base directionally solidified alloy: anisotropy and simulation. Acta Metallurgica et Materialia 1992;40(3):559–67.
- [5] Altenbach H, Huang C, Naumenko K. Creep damage predictions in thin-walled structures by use of isotropic and anisotropic damage models. Journal of Strain Analysis for Engineering Design 2002;37(3):265–75.
- [6] Shesterikov SA, Lokochtchenko AM, Mjakotin EA. Creep rupture of anisotropic pipes. Journal of Pressure Vessel Technology 1998;120(3):223–5.
- [7] Kachanov LM. Time to rupture process under creep conditions. Izv Akad Nank 1958;8:26–31.
- [8] Rabotnov YN. Creep problems in structural members. North Holland: North-Holland Publ. Co; 1969.

- [9] Skrzypek J, Ganczarski A. Modeling of material damage and failure of structures. New York: Springer; 1999.
- [10] Betten J. Creep mechanics. New York: Springer; 2002.
- [11] Altenbach J, Altenbach H, Naumenko K. Edge effects in moderately thick plates under creep damage conditions. *Technische Mechanik* 2004;24(3–4): 254–63.
- [12] Hyde TH, Becker AA, Sun W. Creep damage analysis of short cracks using narrow notch specimen made from a Ni-base superalloy at 700°C. 10th International Conference on Fracture. Honolulu, Oahu, HI. Oxford, UL: Elsevier Science; 2001 Dec 2–6 [International Congress on Fracture].
- [13] Stewart CM, Gordon AP. Modeling the temperature-dependence of tertiary creep damage of a Ni-base alloy. *ASME Early Career Technical Journal* 2008; 7(1):1–8.
- [14] Stewart CM, Gordon AP. Modeling the temperature dependence of tertiary creep damage of a Ni-base alloy. *Journal of Pressure Vessel Technology* 2009; 131(5):1–11.
- [15] Leckie FA, Hayhurst DR. Constitutive equations for creep rupture. *Acta Metallurgica* 1977;25:1059–70.
- [16] Leckie FA, Ponter A. On the state variable description of creeping materials. *Ingenieur Archiv* 1974;43:158–67.
- [17] Hayhurst D, Trampczynski W, Leckie FA. Creep rupture and nonproportional loading. *Acta Metallurgica* 1980;28:1171–83.
- [18] Hyde TD, Sun W, Williams JA. Creep behaviour of parent, weld and HAZ materials of new, service-aged and repaired 1/2Cr1/2Mo1/4V: 2 1/4Cr1Mo pipe welds at 640°C. *Material at High Temperatures* 1999;16(3):117–29.
- [19] MacLachlan DW, Knowles DM. Creep-behavior modeling of the single-crystal superalloy CMSX-4. *Metallurgical and Materials Transactions A* 2000;31(5): 1401–11.
- [20] Batsoulas ND. Creep damage assessment and lifetime predictions for metallic materials under variable loading conditions in elevated temperature applications. *Steel Research International* 2009;80(2):152–9.
- [21] Odquist F, Hult J. *Kriechfestigkeit metallischer Werkstoffe*. Berlin, Germany: Springer; 1962.
- [22] Murakami S, Sanomura Y. Creep and creep damage of copper under multiaxial states of stress. In: Sawczuk A, Bianci G, editors. *Plasticity today*. New York: Elsevier Applied Science Publishers; 1985. p. 535–51.
- [23] Trampczynski WA, Hayhurst DR, Leckie FA. Creep rupture of copper and aluminum under non-proportional loading. *Journal of the Mechanics and Physics of Solids* 1981;29(5–6):353–74.
- [24] Betten J, El-Magd E, Meydanli S, Palmen P. Bestimmung der Materialkennwerte einer dreidimensionalen Theorie zur Beschreibung des tertiären Kriechverhaltens austenitischer Stähle auf der Basis der Experimente. *Archive of Applied Mechanics* 1995;65(2):110–20.
- [25] Murakami S. A continuum mechanics theory of anisotropic damage. In: Boehler JP, editor. *Yielding, damage and failure of anisotropic solids*. London: Mechanical Engineering Publications; 1990. p. 465–82.
- [26] Hayhurst DR. Creep rupture under multi-axial states of stress. *Journal of the Mechanics and Physics of Solids* 1972;20(6):381–2.
- [27] Stewart CM, Gordon AP. Numerical simulation of temperature-dependent, anisotropic tertiary creep damage. 47th AIAA aerospace sciences meeting including the new horizons forum and aerospace exposition. Orlando, FL; Jan 5–8 2009.
- [28] Hyde TH, Sun W. Creep failure behavior of a circumferential P91 pipe weldment with an anisotropic weld metal subjected to internal pressure and end load. *Proceedings of the Institution of Mechanical Engineers, Part L: Journal of Materials Design and Applications* 2006;220(3):147–62.
- [29] Peravali S, Hyde TH, Cliffe KA, Leen SB. Development and use of an anisotropic damage model for the high-temperature life assessment of a P91 weldment. *Journal of Strain Analysis for Engineering Design* 2008;43(5):361–82.
- [30] Peravali S, Hyde TH, Cliffe KA, Leen SB. An anisotropic creep damage model for anisotropic weld metal. *Journal of Pressure Vessel Technology* 2009;131(2):1–8.
- [31] Bhatnagar NS, Gupta RP. On the constitutive equations of the orthotropic theory of creep. *Wood Science and Technology* 1967;1:142–8.
- [32] Hill R. *The mathematical theory of plasticity*. Oxford: Clarendon Press, Oxford Engineering Science Series.
- [33] Murakami S, Ohno N. A continuum theory of creep and creep damage. In: Ponter ARS, Hayhurst DR, editors. *Creep in structures*; 1981. p. 422–43.
- [34] Hyde TH, Jones IA, Peravali S, Sun W, Wang JG, Leen SB. Anisotropic creep behavior of Bridgman Notch specimens. *Proceedings of the Institution of Mechanical Engineers, Part L Journal of Materials: Design and Applications* 2005;219(3):163–75.
- [35] Schur I, Joseph A, Melnikov A, Rentschler R. *Studies in memory of Issai Schur*. New York: Springer; 2003.
- [36] Bernstein DS. *Matrix mathematics*. Princeton, New Jersey: Princeton University Press; 2005. pp. 252–253.
- [37] Schilke PW, Foster AD, Pepe JJ, Beltran AM. Advanced materials propel progress in land-based gas turbines. *Advanced Materials and Processes* 1992; 141(4):22–30.
- [38] Ibanez AR, Srinivasan VS, Saxena A. Creep deformation and rupture behaviour of directionally-solidified GTD 111 superalloy. *Fatigue & Fracture of Engineering Materials & Structures* 2006;29(12):1010–20.
- [39] Sajjadi SA, Nategh S. A high temperature deformation mechanism map for the high performance Ni-base superalloy GTD-111. *Materials Science and Engineering A* 2001;307(1–2):158–64.
- [40] ASTM E-139. Standard test methods for conducting creep, creep-rupture, and stress-rupture tests of metallic materials. No. 03.01. West Conshohocken, PA.
- [41] Gordon AP, Shenoy MM, McDowell DL. Simulation of creep crack growth of a directionally-Solidified Ni-base superalloy. In: proceedings of the 11th international conference on fracture. Turlin, Italy; 2005 March 20–25.
- [42] Peterson LG, Hrencecin D, Ritter A, Lewis N. Hip diffusion bonding of P/M alloys for composite land-based gas turbine buckets. *Progress in Powder Metallurgy* 1986;41:561–78.
- [43] Woodford DA, Frawley JJ. Effect of grain boundary orientation on creep and rupture of In-738 and nichrome. *Metallurgical Transactions* 1974;5(9): 2005–13.
- [44] Sessions ML, McMahon CJ. Influence of stress components on intergranular oxidation and cracking in a nickel-base superalloy. *Nuclear Technology*; 1975:477–89.
- [45] ANSYS Inc. *Theory reference for ANSYS and ANSYS workbench*. Canonsburg, PA: ANSYS Inc.; 2007. pp. 103–105.